Available online at www.sciencedirect.com
SCIENCE DIRECT®
ELSEVIER
Applied Acoustics 65 (2004) 1221–1231
applied acoustics
www.elsevier.com/locate/apacoust

Acoustic intensity measurement of the sound field radiated by a concert harp

F. Gautier *, N. Dauchez

Laboratoire d' Acoustique del' Université du Maine, UMR CNRS 6613, Av. O. Messiaen, 72085 Le Mans cedex 9, France

Received 23 April 2003; received in revised form 21 November 2003; accepted 6 May 2004
Available online 11 September 2004

Abstract

An experimental study of the acoustic radiation of a concert harp is presented. Using a stationary mechanical excitation placed at one string location, the acoustic radiation of the complete instrument is investigated. Two main acoustic radiation sources are identified: the soundboard and the soundbox holes. Acoustic intensity vectors are measured in two planes located in the near field of these two sources, making use of a 3D intensity probe. A detailed description of the acoustic intensity field radiated by these two sources is given. Calculations of acoustic power radiated by the soundboard surface and by the soundbox holes allow us to quantify the relative importance of these two sources. In three frequency ranges, it is shown that the soundbox holes radiate more than the soundboard. In the first range, it is suggested that the acoustic radiation of the instrument can be described by two point sources of sound implying that in this range the harp acts as an equivalent elastic Helmholtz resonator.

Keywords: Harp; Acoustic radiation; Acoustic intensity measurement

* Corresponding author. Tel.: +33 2 43 83 39 81; fax: +33 2 43 83 37 94.
E-mail address: Francois.Gautier@univ-lemans.fr (F. Gautier).

0003-682X/$ - see front matter
doi:10.1016/j.apacoust.2004.05.006

1. Introduction

Stringed musical instruments generally comprise many couplings and consequently their acoustic radiation can be quite complex. In the case of instruments such as the guitar and the violin, the acoustic radiation has been extensively investigated [1,2], but there are relatively few studies related to the harp, despite the fact that it works in a similar way. The harp (see Fig. 1) is composed of a tapered, stiffened, roughly trapezoidal thin plate, called the soundboard. The soundboard is fixed on a thick cone shaped cavity, called the soundbox, and is excited by strings attached from the central line of the soundboard to the string arm. A column, called the pillar, connects the string arm and the base of the soundbox and allows the soundboard to withstand the strings' tension. Several holes are cut into the underside of the soundbox to permit access to the back of the soundboard for string mounting. These holes also permit the soundboard to radiate sound through the back of the instrument, but, unlike with the guitar, they are not designed to take advantage of the Helmholtz resonator effect for sound amplification in the low frequency range.

Relatively few studies have been carried out that relate to the acoustic radiation from the harp. Using the Chladni glitter pattern method, experimental modal analysis of a small harp of Scotland, called the clarsach, was performed at different stages of the construction of the instrument: free soundboard, ribbed soundboard, complete instrument [3,4]. In these studies, several vibratory modes of the soundboard were obtained. An input admittance map was also measured, to investigate the ability of a string to excite a soundboard mode, depending on its location and

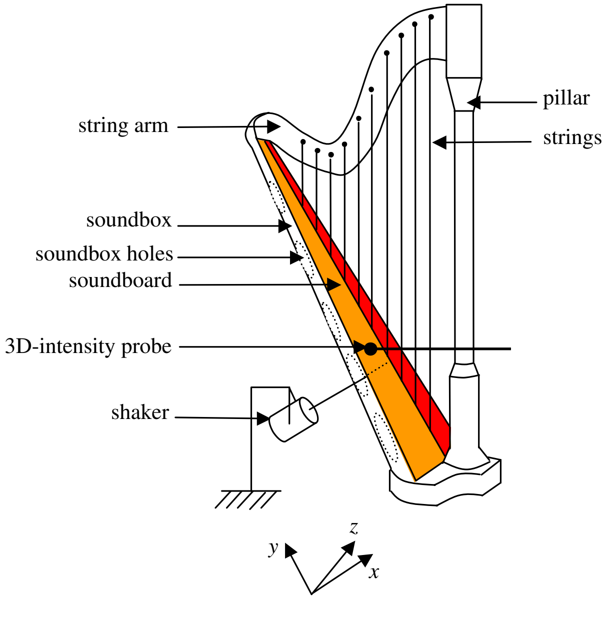

Fig. 1. Experimental set-up.

its fundamental frequency. The relationship between the vibration modes of the instrument and the radiated sound was not investigated. More recently [5], a modal analysis of a composite Pandora harp was performed using laser vibrometer measurements on the complete structure (soundboard and soundbox). In the frequency range studied (0–500 Hz), 13 experimental modes of the soundbox were identified. From the measured modal shapes, it was shown that the displacement amplitudes of the soundbox can be of the same order of magnitude as those of the soundboard. Comparison between a modal basis calculated using the finite element method and the experimental modes showed a good agreement in terms of mode shape and frequencies for six of these modes. The influence of the fluid located inside the cavity and the influence of the strings on the soundboard modes were not taken into account in the numerical simulations. The relationships between the structural modes and the acoustic radiation were also not investigated. Some aspects of these relationships were, however, studied experimentally and numerically for the case of a celtic harp [6]. Using a shaker to provide a stationary excitation, acoustic pressure was measured on a cylindrical mesh around the instrument (non-baffled configuration). These acoustic pressure measurements were then compared with predictions based on the boundary element method, with measurement of the normal velocity of the soundboard being used as input data for calculating the radiated sound. For this calculation, the radiation surface was assumed to be inserted in an infinite plane and rigid baffle. A qualitative agreement was obtained for frequencies for which the soundbox vibration level was low compared with the soundboard radiation level. In order to study the vibroacoustic couplings which occur on the complete instrument, an analytical model was developed using a simplified configuration [7]. In this model, the soundbox is assumed to be a parallelepiped shaped cavity and the soundboard is assumed to be a rectangular simply supported plate excited at one point by a harmonic force. Rigid baffles are introduced in the soundboard plane and in the plane of the soundbox holes in order to obtain an analytically tractable solution. In such a model, the introduction of rigid baffles leads to an artificial separation of the soundboard radiation and the radiation from the soundbox holes. The validity of this strong approximation should be tested using appropriate experiments.

The aim of this study is to provide a description of the acoustic radiation of a concert harp, based on acoustic intensity measurements, in order to identify the main acoustical sources. Such experimental results can also be used to validate numerical or analytical models which will be developed in the future. Presentation of the experimental set up and results related to the acoustic intensity field are provided in Sections 2 and 3, respectively.

2. Experimental procedure

A diagram of the experimental set up used in this study is shown in Fig. 1. A Camacs concert harp (Model Atlantide Prestige, Serial No. 2000.294) was excited using a shaker which was connected to the soundboard by a stinger. The shaker was positioned on the central line of the soundboard close to the A2 string (fundamental frequency 110 Hz) and provided a broadband noise excitation. Acoustic intensity vector measurements were then made using a 3D intensity probe comprising four 1/4'' microphones arranged in a 2.5 cm side tetrahedron. The acoustic intensity vector, that is the acoustic power per unit surface area, is calculated from the product of acoustic pressure and acoustic velocity. Acoustic pressure is the mean pressure over the four microphones. Acoustic velocity components are determined from the differences of pressure of the three pairs of microphones. In order to increase the accuracy in the low frequency range, the microphones were calibrated in pairs using a small cavity. The harp was placed on the floor of a semi-anechoic chamber, providing a low noise environment over the frequency range of interest (100–1000 Hz). It should also be noted that in order to damp the strings' vibrations, paper (towel) was inserted between the strings.

By controlling the intensity probe using an automated displacement system, measurements of acoustic intensity were obtained at different positions on two surfaces. These measurement surfaces are depicted in Fig. 2, where the orientation of the axes is such that the z axis is normal to the plane of the soundboard. The first measurement surface – the front surface, denoted by S_{front} is a rectangular area located 1 cm above the soundboard. It is divided into two domains: the half soundboard S_{board}, whose area is 0.18 m^2 and a complementary surface, the exterior surface S_{ext}, whose area is 0.13 m^2. The surfaces S_{board} and S_{ext} cover only half of the soundboard plane, taking advantage of the symmetry about the plane of the strings. The front surface is meshed by a 8×15 grid of measurement points. The second measurement surface, denoted by S_{holes}, is a rectangular surface of area 0.06 m^2, located 1 cm above the plane of the soundbox holes. The two measurement planes are located very close to the soundboard and to the surface containing the sound box holes, to be sure that the acoustic power which crosses these planes is solely due to the soundboard and to the soundbox holes, respectively. The hole surface is meshed only by 1 line of 21 measurement points. We denote the five holes of the instrument from 1 to 5 as shown in Fig. 2.

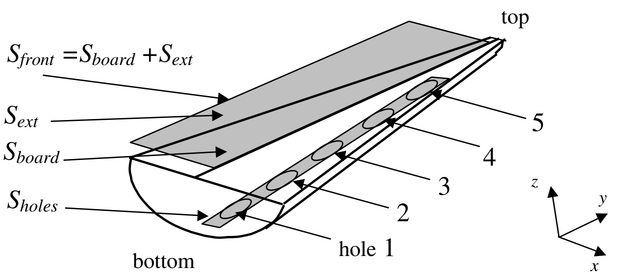

Fig. 2. Definition of the measurement surfaces.

3. Experimental results

3.1. Acoustic power radiated by the soundboard and the soundbox holes

Analysis of the acoustic powers radiated through the surfaces S_{board} and S_{holes} is performed in order to identify useful frequency ranges. Integration of the normal acoustic intensity vector through one surface S provides the acoustic power radiated through this surface [8]

$$\Pi_S = \int_S \vec{I}\,\mathrm{d}\vec{S} \cong \sum_i I_k \Delta S_k \cong S\langle I\rangle_S, \tag{1}$$

where $\langle I\rangle_S$ is the average normal intensity on the surface S. This relation is applied to define the acoustic power radiated by the soundboard $\Pi_{\text{board}} = 2S_{\text{board}}\,\langle I\rangle_{\text{board}}$ and by the holes $\Pi_{\text{holes}} = S_{\text{holes}}\,\langle I\rangle_{\text{holes}}$. The factor 2 is introduced because measurements are performed on the half soundboard bounded by the plane of the strings. Preliminary tests have shown that the vibration level measured on the soundbox is sufficiently low compared with the vibration level measured on the soundboard that it can be assumed that the acoustic power radiated by the soundbox is negligible compared to the acoustic powers radiated by the soundboard and the holes. Therefore, the total power radiated by the instrument is $\Pi_{\text{total}} = \Pi_{\text{board}} + \Pi_{\text{holes}}$.

In Fig. 3, the measured acoustic powers Π_{holes} and Π_{board} are plotted versus frequency. A thick line below the frequency axis is plotted when Π_{board} takes higher values than Π_{holes}. This indicator leads to the definition of six frequency ranges, denoted by A–F in Fig. 3. In the ranges A (100–220 Hz), C (409–471 Hz) and E (491–553 Hz), the acoustic power radiated by the soundbox holes is greater than the acoustic power radiated by the soundboard. In the ranges B (220–409 Hz), D (471–491 Hz) and F

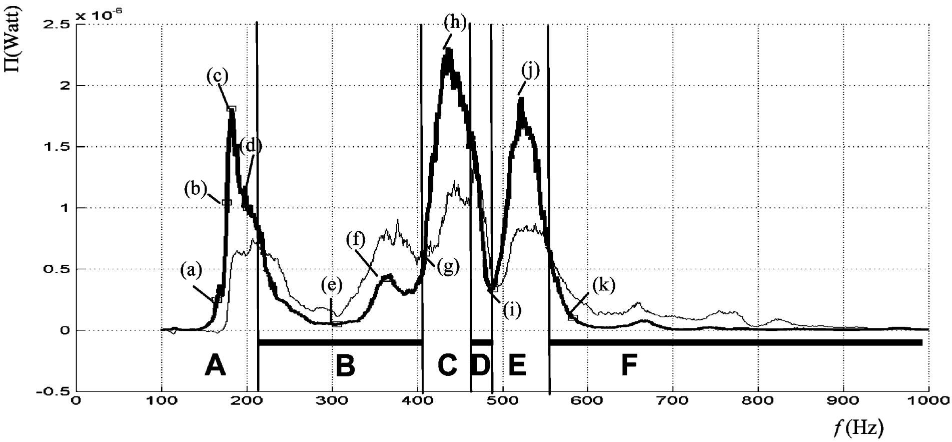

Fig. 3. Acoustic power radiated by the soundboard surface (thin line), and by the soundbox holes (thick line). In the frequency ranges A, C and E, acoustic power radiated by the soundbox holes is greater than acoustic power radiated by the soundboard. In the frequency ranges B, D and F, the opposite result is observed. Selected frequencies (a)–(k) are related to subfigures of Fig. 5.

(553–1000 Hz), the opposite result is observed. Such measurements show the importance of the contribution of the soundbox holes to the total radiated acoustic power.

In Fig. 4, acoustic power is plotted in configurations, where the soundbox holes are opened or closed by heavy bitumen sheets. It is shown that for almost all frequencies (some frequencies near the particular value of 200 Hz being excepted), the total acoustic power radiated by the instrument is greater when the instrument works in a normal way (open holes). Although the soundbox holes were originally not designed for sound radiation but for string mounting, they do cause an increase in the total radiated power, especially in the frequency ranges A, C and E.

3.2. Spatial distribution of acoustic intensity vectors

Representative spatial acoustic intensity distributions measured on the front surface, and on the holes surface are shown in Fig. 5 for selected frequencies. These particular frequencies, which are also indicated in Figs. 3 and 7, allow us to illustrate some typical results. Several conclusions can be drawn:

1. Spatial acoustic intensity distribution is not uniform over the instrument. In the low frequency range A (Fig. 5(a)–(d)), the magnitudes of the acoustic intensity vectors reach maximum values in the bottom part of the instrument (bottom part of the soundboard and holes 1, 2). The location of this maximum tends to be shifted to the higher part of the instrument (higher values of y) at higher frequencies (Fig. 5(f)–(j)).

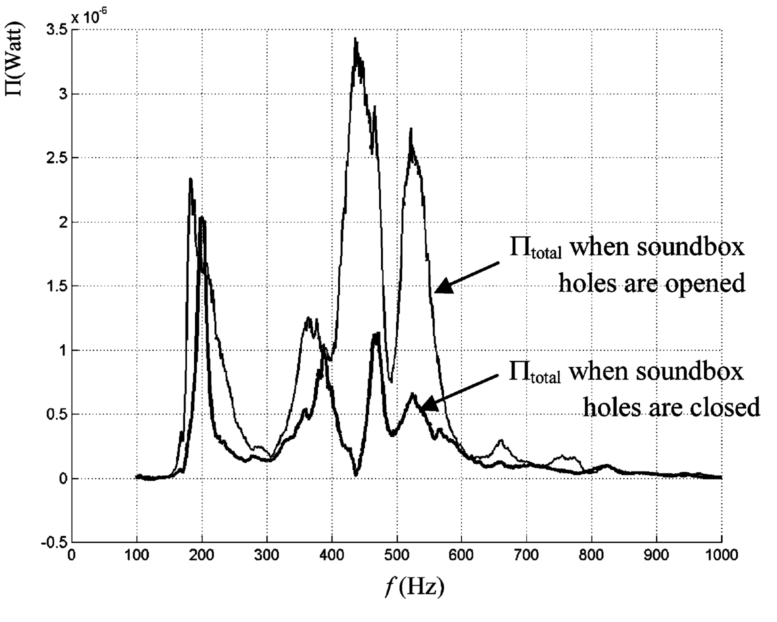

Fig. 4. Total acoustic power radiated by the instrument when the soundbox holes are opened (thin line) and closed (thick line).

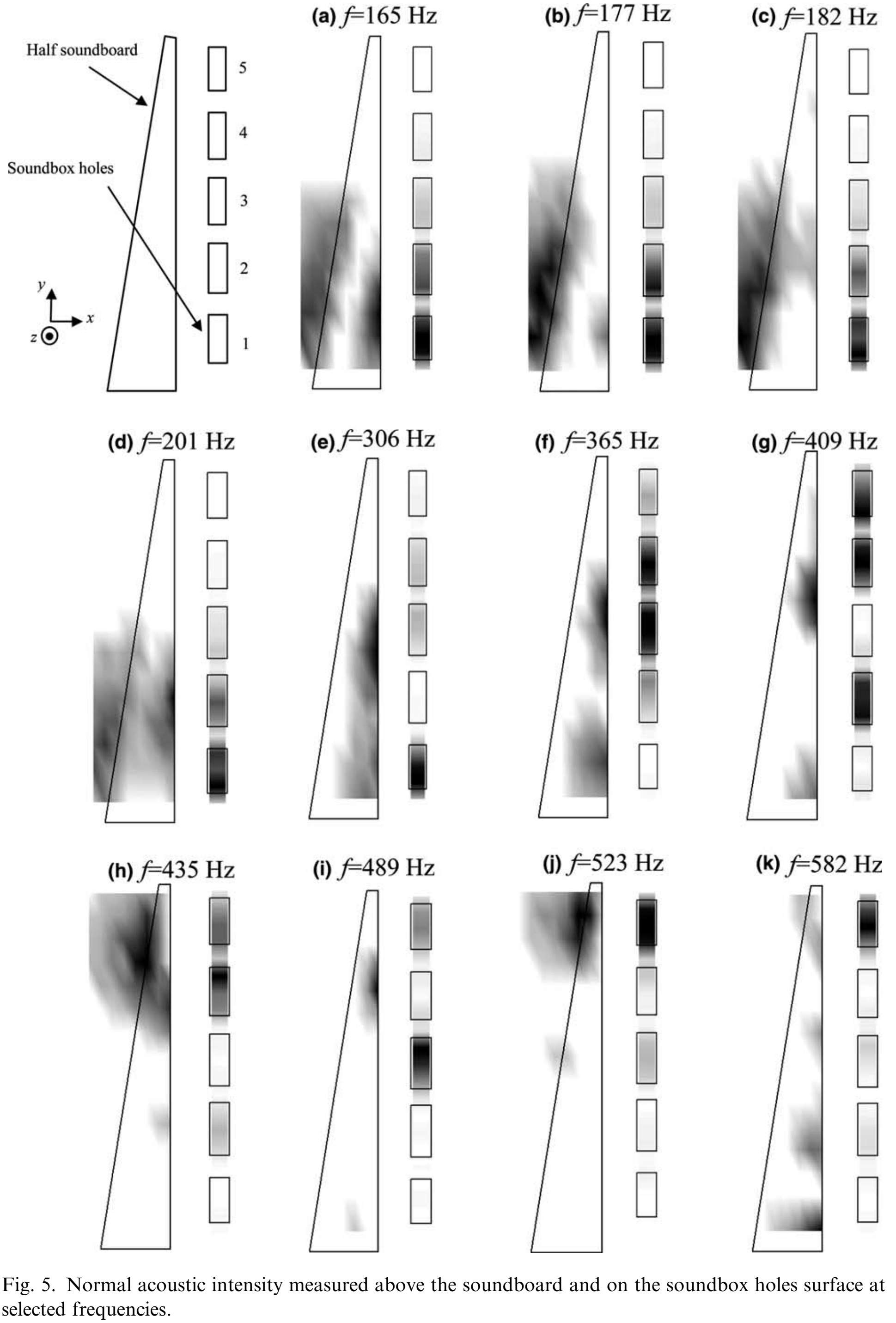

Fig. 5. Normal acoustic intensity measured above the soundboard and on the soundbox holes surface at selected frequencies.

2. The number of distinct acoustic radiation areas on the soundboard increases with frequency: one area is observed in range A (Fig. 5(a)–(d)), 2 or 3 in ranges B, C, D, E (Fig. 5(f)–(j)) and 4 in range F (Fig. 5(k)).
3. In frequency ranges A, C and E, where the acoustic radiated power of soundbox holes dominates, acoustic intensity vectors on the exterior surface have significant amplitudes (Fig. 5(a)–(d), (h) and (j)). This is due to the radiation of the holes towards the front face of the harp.

3.3. Radiation of the instrument in the low frequency range

In the first frequency range (Range A: 100–220 Hz), it is mainly the bottom part of the soundboard and holes 1–2 that radiates. In this case, it is convenient to analyse the intensity field as resulting from a superposition of two point sources of sound: the first would be located on the bottom part of the soundboard, and the second on the area of the holes 1–2. The variations of the intensity vector distributions observed between Fig. 6(a) and (c) show that the relative magnitude and phase of these two sources depend on frequency.

In Fig. 6(a) corresponding to $f = 165$ Hz, the intensity vectors on the soundboard have high amplitudes and are mainly orientated towards the instrument (in the ingoing normal direction, denoted by $-z$). On the surface of the soundbox holes, intensity vectors are orientated in the $-z$ direction, which is the outgoing normal direction. These two orientations show that the instrument is radiating like two equivalent point sources of sound having different acoustic flows (amplitude and phase). Such a configuration is observed for frequency values between 160 and 177 Hz. Note that the radiation from the soundbox holes leads to an orientation of the intensity vectors in the $+z$ direction on the exterior surface S_{ext}.

In Fig. 6(c) corresponding to $f = 182$ Hz, the same configuration as the previous one is shown: in this case, the acoustic intensity vectors on the soundboard have high amplitudes but are orientated in the outgoing direction ($+z$). The relative amplitude and phase between the two equivalent point sources of sound have changed in comparison with the configuration for $f = 165$ Hz. An intermediate case is presented in Fig. 6(b): in this case, the intensity vectors on the soundboard surface have amplitudes close to zero.

In the three presented cases (Fig. 6(a)–(c)), it is shown that the part of the front surface where the magnitude of the intensity vectors is maximum is not located on the soundboard but on the exterior surface. This observation shows that the radiation of the soundbox holes is important enough to lead to an orientation of the intensity vector in the $+z$ direction for the exterior surface.

A magnified section of the curves presented in Fig. 3 is shown in Fig. 7. It is seen that the acoustic power radiated by the holes reaches local maxima at $f = 168$ and 182 Hz. It can be suggested that these maxima correspond to the two resonances of an elastic Helmholtz resonator. Such a model is commonly used to describe the behaviour of the guitar, which is similar to a bass-reflex enclosure in the low frequency range [9,10]. In a more general way, it has been shown that in the low fre-

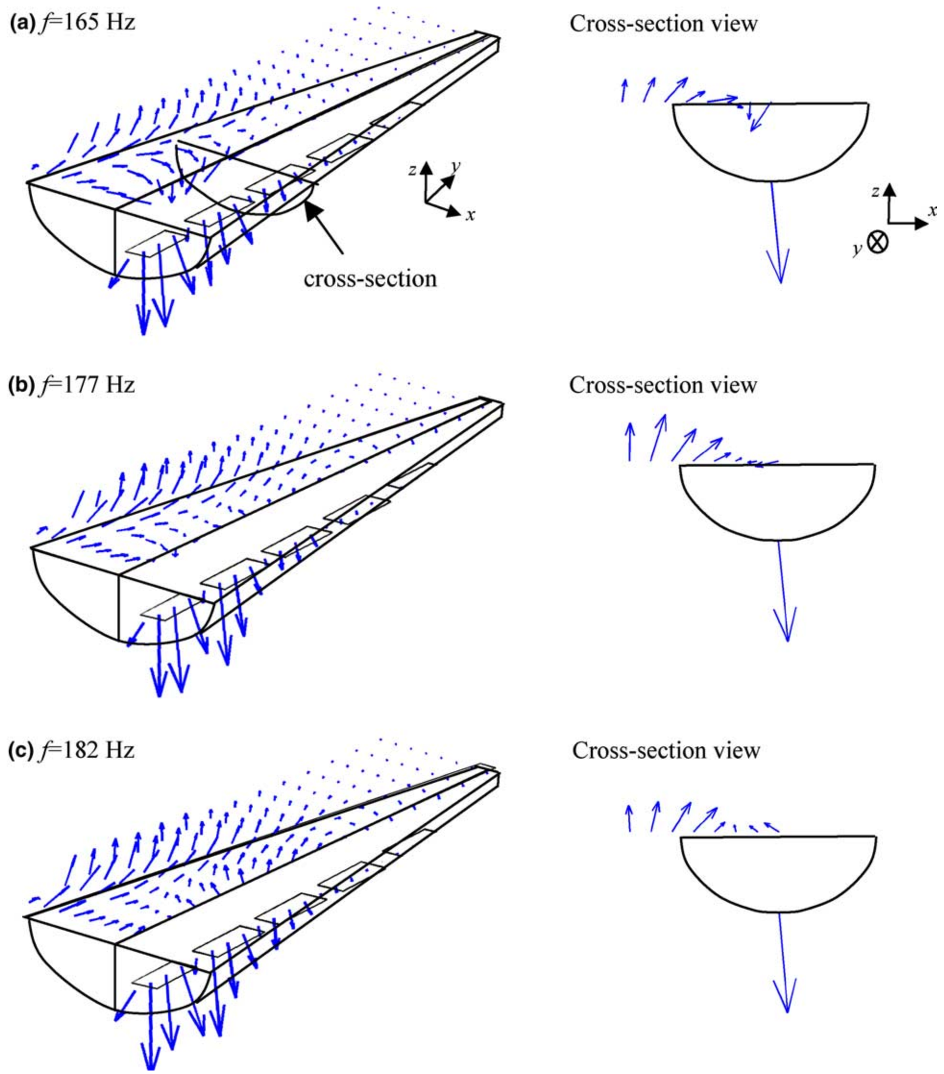

Fig. 6. Intensity vector distribution measured on the soundboard (front surface) and near the soundbox holes at selected frequencies (a)–(c). Details of the intensity vector distribution on the cross-section are also shown for the same frequencies.

quency range, the radiation pattern of a string instrument that has a sound hole in its shell is that of a dipole [11]. Such a result can be obtained using a multipole expansion of the sound field outside a sphere which encloses the source. In such a configuration, a two degrees of freedom model can be used to describe the oscillators representing the first top-plate resonance and the Helmholtz air resonance. The two mechanical oscillators act like acoustic flow sources and lead individually to

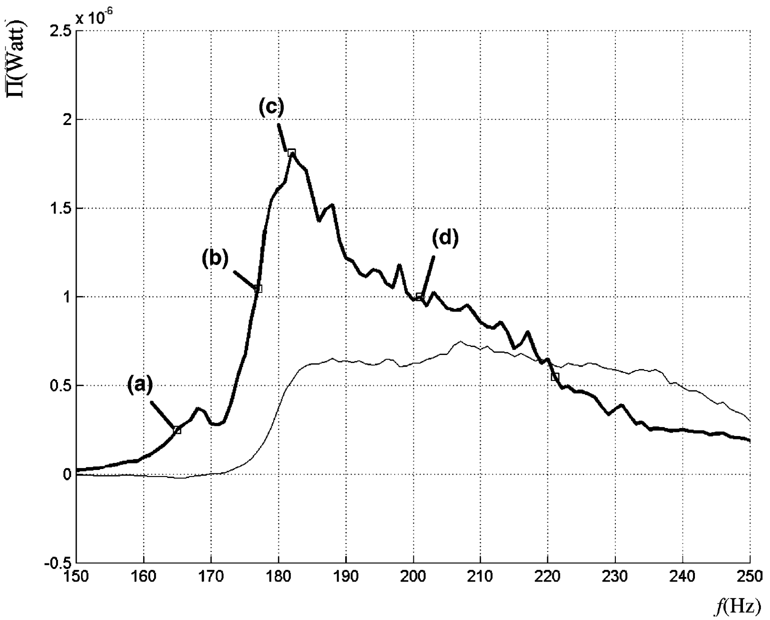

Fig. 7. Acoustic power radiated by the soundboard surface (thin line) and by the soundbox holes (thick line).

monopole acoustic radiation. In the case of the harp, definition of the equivalent elastic Helmholtz resonator is not so easy as in the case of the guitar because of the existence of multiple soundbox holes.

4. Conclusion

The acoustic radiation of a concert harp has been investigated using intensity vector measurements. Comparison of the acoustic radiated power of the soundbox holes and the soundboard shows that the soundbox holes do cause an increase in the total radiated power, especially in frequency ranges A, C and E, despite the fact that they were not originally designed for sound radiation but instead for string mounting. The two types of acoustic source interact over the whole frequency range. Analysis of the spatial distributions of intensity vectors shows that the bottom part of the instrument radiates mainly in the low frequency range, whereas the upper part radiates mainly at high frequencies. The number of distinct acoustic radiation areas also increases from 1 to 4 with frequency.

In the low frequency range (100–220 Hz), it is suggested that acoustic radiation can be described by two equivalent point sources of sound. Their relative amplitudes and phases can be determined by a two degrees of freedom system describing the harp as an equivalent elastic Helmholtz resonator. This approach has been successfully used to describe the behaviour of the guitar in the low frequency range. Its application to the harp is not straightforward because of the presence of several holes and will be the subject of following works.

Acknowledgements

The authors thank the luthier CAMAC harps for its interest in the study and for having lent an instrument, the Institut Technique Européen des Métiers de la musique (ITEMM), Le Mans, the Centre de Transfert de Technologie du Mans (CTTM), especially J.-L. Mary, where the measurements were performed, J. Gilbert and V. Doutaut for helpful discussions, and J.-L. Le Carrou and B. Massol (students at Ecole Nationale Supérieure d'Ingénieurs du Mans) for their participation in this work.

References

[1] Richardson BE. Stringed instruments: plucked. In: Malcom J Crocker, editor. Encyclopedia of acoustics; 1997 [chapter 132].
[2] Fletcher NH, Rossing TD. The physics of musical instruments. Berlin: Springer; 1991.
[3] Firth M. On the acoustics of the harp. Acustica 1977;37:148–54.
[4] Bell AJ. An acoustical investigation of the concert harp. PhD thesis. University of St. Andrews, UK; 1987.
[5] Kergoulay G, Balmes E. Dynamic behaviour of a harp soundboard and soundbox. In: Proceedings of the international conference on information systems, analysis and synthesis, SCI/ISAS, July 2001, Orlando (FL), USA.
[6] Le Pichon A. Méthode de prédiction du rayonnement acoustique de structures volumiques composées d'une ou plusieurs faces planes vibrantes. Application aux instruments de musique à cordes [text in French]. PhD thesis, Université de Paris XI, France; 1996.
[7] Bareau L. Modélisation vibroacoustique d'une harpe simplifiée [text in French]. Master (DEA) report, Université du Maine, Le Mans, France; 2002.
[8] Fahy FJ. Sound intensity. 2nd ed. 1995. London: E&FN SPON.
[9] Christensen P, Vistisen Bo B. Simple model for low-frequency guitar function. J Acoust Soc Am 1980;68(3):758–66.
[10] Firth IM. Physics of the guitar at the Helmholtz and first top-plate resonances. J Acoust Soc Am 1977;6(2):588–93.
[11] Weinreich G. Sound hole sum rule and the dipole moment of the violin. J Acoust Soc Am 1985;77(2):710–8.